Journal of Chemical Learning Innovation
Vol. 1, No. 2, December 2024, pp. 86~95
ISSN: 3063-0886, DOI:10.37251/jocli.v1i2.3001

Exploration of the Structure and Composition of $Sn(S_{0.6}Te_{0.4})$ Thin Film as a Potential Absorber in Solar Cell Technology

Mahmudah Setianingrum[1], and Guluzra Bozorboeva[2]
[1]Department of Physics Education, Universitas Negeri Yogyakarta, Yogyakarta, Indonesia
[2]Department of Chemical Engineering, Institute of Polymer Chemistry and Physics, Tiongkok

Article Info

Article history:

Received Oct 3, 2024
Revised Nov 15, 2024
Accepted Dec 9, 2024
OnlineFirst Dec 31, 2024

Keywords:

Chemical Composition
Crystal Structure
$Sn(S_{0.6}Te_{0.4})$ Thin Film
Solar Cell Absorber
Vacuum Evaporation

ABSTRACT

Purpose of the study: This study aims to synthesize and characterize $Sn(S_{0.6}Te_{0.4})$ thin films using vacuum evaporation and to analyze their crystal structure and chemical composition in order to evaluate their potential as absorber materials for solar cell applications.

Methodology: Vacuum evaporation system with rotary and diffusion pumps, substrate heater, Penning manometer, thermocouple, furnace, digital balance, and multimeter were used. Structural analysis employed X-Ray Diffraction (Miniflex 600 Rigaku, Cu source). Surface morphology and composition were analyzed using Scanning Electron Microscopy (SEM) and Energy Dispersive Spectroscopy (EDS). Data processed using Origin and PCPDFWIN software.

Main Findings: $Sn(S_{0.6}Te_{0.4})$ thin films were successfully deposited at 250°C, 300°C, and 350°C. XRD results show increased diffraction peak intensity with higher temperature, indicating improved crystallinity, with optimum at 350°C. The structure approaches orthorhombic SnS. EDS confirms presence of Sn, S, and Te with composition close to theoretical values but slightly deviated due to non-stoichiometric effects.

Novelty/Originality of this study: This study explores a specific composition of $Sn(S_{0.6}Te_{0.4})$ thin film using vacuum evaporation and simultaneously analyzes its crystal structure and chemical composition. It provides new insight into the relationship between temperature, crystallinity, and composition, contributing to the development of alternative absorber materials for solar cell technology.

Corresponding Author:
Mahmudah Setianingrum,
Department of Physics Education, Universitas Negeri Yogyakarta, Jl. Colombo No.1 Karangmalang Yogyakarta, Indonesia
Email: mhmdstningrum00@gmail.com

1. INTRODUCTION

The development of renewable energy technology is increasingly becoming a major focus in addressing the global energy crisis and climate change issues [1], [2]. One of the most promising technologies is solar cells due to their ability to directly convert solar energy into electrical energy [3], [4]. Absorbent materials play a crucial role in determining solar cell efficiency [5], [6]. Therefore, exploring new materials with optimal optical and electronic properties is crucial. One approach is to utilize materials based on chalcogenide compounds.

Chalcogenide materials such as sulfides and tellurides have been extensively studied due to their excellent optical properties and suitable band gaps for photovoltaic applications [7], [8]. The combination of sulfur (S) and tellurium (Te) in a single material allows for more flexible engineering of electronic properties [9], [10]. The compound $Sn(S_{0.6}Te_{0.4})$ is a potential candidate as an absorber in solar cells. This composition is expected to

achieve a balance between material stability and light absorption efficiency. Therefore, studying this material is relevant for further development [11], [12].

Thin films are a common material form used in solar cell technology due to their efficiency in material use and ease of fabrication [13], [14]. Vacuum evaporation is a widely used method for producing high-quality thin films [15], [16]. This method allows for fine control over material thickness and composition. Furthermore, it is relatively simple and can produce homogeneous films [17], [18]. Therefore, vacuum evaporation was chosen as the approach in this research.

Characterizing the structure and chemical composition is a crucial step in understanding the fundamental properties of thin film materials [19], [20]. The resulting crystal structure influences the optical and electrical properties of the material [21], [22]. Meanwhile, the chemical composition determines the stoichiometry, which influences the material's performance [23], [24]. Therefore, an in-depth analysis of both aspects is essential. The results of this characterization will provide insight into the material's potential as a solar cell absorber.

Although various studies have been conducted on SnS and SnTe materials separately, studies on Sn(S,Te) alloys are relatively limited. Previous research has generally focused on optical or electrical properties without comprehensively examining the relationship between structure and composition [25], [26]. Furthermore, certain composition variations, such as $Sn(S_{0.6}Te_{0.4})$, have not been thoroughly explored. This indicates a research gap that needs to be filled. Therefore, a more integrated study is needed to understand the characteristics of this material.

The novelty of this research lies in exploring the specific composition of $Sn(S_{0.6}Te_{0.4})$ synthesized using a vacuum evaporation technique. This research also simultaneously examines the relationship between crystal structure and chemical composition. This approach is expected to provide a more comprehensive understanding of material properties [27], [28]. Furthermore, this research has the potential to contribute to the development of new absorber materials. Thus, this research has added value compared to previous studies.

The urgency of this research is based on the need for efficient, stable, and environmentally friendly solar cell materials. The development of Sn(S,Te)-based materials is expected to be an alternative to expensive and toxic conventional materials. Furthermore, optimizing the material composition can improve energy conversion efficiency. This research also supports efforts to develop sustainable renewable energy. Therefore, the results of this study are expected to make a significant contribution to the field of photovoltaic technology.

2. RESEARCH METHOD

2.1. Research Materials and Equipment

The materials used in this study consisted of several key components that support the semiconductor thin film preparation process. The base materials used were tin (Sn), sulfur (S), and tellurium (Te) powder, which form the $Sn(S_{0.6}Te_{0.4})$ compound. Furthermore, a 1 mm thick glass substrate served as the thin film growth medium. To ensure the cleanliness of the substrate surface, cleaning agents such as water, soap, alcohol, and tissue were used. All materials were carefully prepared to ensure optimal deposition quality.

The equipment used in this study included a preparation device and a characterization device for the $Sn(S_{0.6}Te_{0.4})$ semiconductor material. The preparation process was carried out using a vacuum evaporation system as the primary tool in thin film formation. This system was supported by a vacuum pump consisting of a rotary baffle pump for initial pressure and a diffusion pump to achieve a lower vacuum pressure. Furthermore, a substrate heater equipped with a slide regulator controlled the temperature during the deposition process [29]. Pressure measurements in the vacuum chamber were performed using a Penning manometer, while substrate temperature was monitored using a thermocouple.

Additional equipment included a furnace used to preheat the glass substrate prior to the deposition process. The mass of the semiconductor material was determined using a high-precision digital balance. During the heating process, the voltage was measured using a digital multimeter to ensure stable operational conditions. The evaporation time was controlled using a stopwatch to obtain parameters appropriate to the research requirements. This combination of equipment allowed the preparation process to proceed in a controlled and systematic manner.

In addition to the preparation equipment, this study also utilized various characterization instruments to analyze the properties of the resulting materials. X-Ray Diffraction (XRD) was used to identify the crystal structure and determine the lattice parameters of the $Sn(S_{0.6}Te_{0.4})$ thin films. Scanning Electron Microscopy (SEM) was used to observe the surface morphology, which is capable of producing high-resolution images. Meanwhile, the chemical composition of the material was analyzed using Energy Dispersive Spectroscopy (EDS). These three techniques complement each other in providing comprehensive information about the characteristics of the resulting materials.

2.2. Research Steps

This research procedure was carried out through several systematic stages, starting with material preparation. In this stage, the main material, the $Sn(S_{0.6}Te_{0.4})$ compound, was prepared for the deposition process. The glass substrate was cleaned using detergent and alcohol to remove impurities that could affect the quality of the thin film. Next, the substrate was heated in a furnace at 100°C to remove any remaining moisture. The semiconductor material was then weighed at 0.25 grams using a digital scale. The material was then loaded into a crucible in the evaporator system, followed by installation of a spacer, placement of the substrate in the holder, installation of the substrate heater, connection of cables to the slide regulator, and tight closure of the chamber.

The next stage was material preparation using a vacuum evaporation technique. The process began by activating the rotary pump as the primary pump to create an initial vacuum. The system was then set to the rough valve position and left to stand for several minutes. Next, the diffusion pump was turned on as the secondary pump with a specific voltage setting to achieve a lower vacuum pressure. The valves in the system were operated in stages, including adjusting the back valve and bypass valve to stabilize the vacuum. The pressure in the chamber was monitored using a Penning manometer until a stable condition was achieved. Once the vacuum was achieved, the substrate heater was activated and set at various temperatures: 250°C, 300°C, and 350°C.

Once the desired pressure and temperature reached the desired levels, the evaporation process began by heating the material in the crucible until it evaporated and deposited on the substrate surface [30]. This process was controlled using a slide regulator to ensure optimal evaporation. Once all the material had evaporated, the system was gradually shut down by resetting the voltage to zero and turning off related devices, such as the thermocouple. The system valves were then closed according to procedure and the Penning manometer was turned off. The diffusion pump cooled for approximately 45 minutes before the system was completely shut down. This stage concluded by turning off all pumps used in the system.

The next step was to collect the thin film preparation results. This process began by normalizing the air pressure in the chamber by relaxing the available valves. The chamber is then opened and removed from its mounting to collect the sample. Components such as the substrate heater and holder are carefully removed to avoid damaging the thin film. The deposited sample is then removed and stored in a sealed container to prevent oxidation. Once the sampling process is complete, the chamber is tightly closed again to maintain the instrument's condition.

2.3. Characterization Stage of the Preparation Material

The characterization phase was carried out to identify the structural properties and composition of the prepared $Sn(S_{0.6}Te_{0.4})$ thin films. The first characterization was performed using X-Ray Diffraction (XRD) techniques using a Miniflex 600 Rigaku instrument equipped with a Cu tube with an X-ray wavelength of 1.54060 Å. This technique aims to determine the crystal structure and lattice parameters of the thin films produced by the vacuum evaporation method. The characterization process begins with preparing the samples to be tested, then mounting them in the XRD instrument's specimen chamber. After the measurement process is complete, the diffraction data are printed and analyzed to identify the crystal phases formed.

In addition to XRD, characterization was also performed using Scanning Electron Microscopy (SEM) and Energy Dispersive Spectroscopy (EDS). SEM is used to observe the surface morphology of the thin films to obtain information in the form of high-resolution images. Meanwhile, EDS is used to determine the chemical composition of the material through analysis of the elemental spectra contained in the samples. These two techniques complement each other in providing a comprehensive picture of the physical and chemical characteristics of the material. Thus, the characterization results can be used to evaluate the quality of the resulting thin film.

The SEM and EDS characterization process begins with cutting the prepared sample to the required size. The sample is then attached to a holder using conductive glue to ensure good electrical contact during observation. Next, the sample is heated using a water heater to dry the conductive glue and ensure complete adhesion. Afterward, the sample surface is cleaned of dust using a hand blower to avoid interfering with the observation results. The prepared sample is then placed in the specimen chamber of the SEM and EDS instruments for analysis.

During the observation stage, specific areas of the sample are selected for detailed observation using the SEM. This process produces surface morphology images that reveal characteristics such as grain size and layer homogeneity. Simultaneously, EDS analysis is performed to obtain elemental composition data in the form of spectra. The resulting data is then recorded and stored in a file for further analysis. Through this step, comprehensive information is obtained regarding the surface structure and chemical composition of $Sn(S_{0.6}Te_{0.4})$ thin films.

2.4. Data Analysis Techniques

The data analysis technique in this study began with processing the X-Ray Diffraction characterization results in the form of diffractograms. These diffractograms display the relationship between intensity and the diffraction angle (2θ), which serves as the basis for identifying the material's crystal structure. The measured data were then compared with standards from the Joint Committee on Powder Diffraction Standards database to

determine the crystal planes (hkl) formed. Next, lattice parameters, such as a, b, and c, were calculated using analytical methods based on the obtained diffraction data. This analysis enabled the evaluation of the crystal structure of each sample.

The diffractogram results and lattice parameters from several samples were then compared to determine the effect of variations in substrate temperature on the resulting crystal structure. This comparison provides an overview of the optimum conditions in the thin film preparation process. Thus, the sample with the best crystal quality can be determined based on the sharpness of the diffraction peaks and its agreement with the standard data. The best sample was then selected for further characterization. This approach aims to obtain more focused and in-depth analysis results.

Further analysis was performed using Scanning Electron Microscopy to observe the surface morphology of the thin film. The data obtained consisted of images showing the shape, size, and distribution of grains on the material's surface. From these images, the homogeneity and density of the resulting thin film structure can be analyzed. This information is crucial for determining the film's quality as an absorbent material. Furthermore, SEM results provide a visual representation that supports the interpretation of crystal structure data.

Next, characterization using Energy Dispersive Spectroscopy was performed to determine the material's chemical composition. Energy Dispersive Spectroscopy data is displayed in the form of a spectrum, demonstrating the relationship between the intensity and energy of the detected signal. This spectrum allows the elements present in the sample to be identified. Furthermore, the percentage composition of each element can be calculated to ensure compliance with the planned initial composition. Thus, Energy Dispersive Spectroscopy analysis provides additional information regarding the chemical properties of the resulting material.

3. RESULTS AND DISCUSSION

3.1. Characterization of Crystal Structure and Lattice Parameters of XRD (X-Ray Diffraction) Results

X-Ray Diffraction (XRD) characterization in this study was used to identify the crystal structure and determine the lattice parameters of a thin film of $Sn(S_{0.6}Te_{0.4})$ produced by vacuum evaporation. The XRD measurement results are in the form of a diffractogram showing the relationship between the scattering angle (2θ) and the intensity (I) of the diffraction peaks. The recorded intensity reflects the number of signals received by the detector during the measurement process. This diffraction pattern serves as the basis for determining the crystal phase and the orientation of the crystal planes (hkl). Thus, XRD characterization provides fundamental information regarding the structure of the resulting material.

This characterization process used a copper (Cu) radiation source with a wavelength (λ) of 1.54056 Å. Measurements were carried out under operating conditions with a voltage of 40 kV and a current of 15 mA to produce stable X-rays. The observed diffraction angle (2θ) ranges from 0° to 90°, allowing identification of the various diffraction peaks that appear. This parameter setting is crucial for obtaining accurate and representative data on the material's crystal structure. Under these conditions, the diffractogram results can be optimally analyzed.

The diffraction patterns produced from $Sn(S_{0.6}Te_{0.4})$ thin films show characteristic variations based on the substrate temperature used during the preparation process. Samples prepared at 250°C, 300°C, and 350°C produce different diffraction patterns, both in terms of peak position and intensity. These differences indicate changes in the crystal structure and degree of crystallinity of the material. Further analysis of the diffraction peaks can be used to determine the dominant crystal plane. Thus, variations in substrate temperature influence the structural properties of the thin films.

The diffractogram results for each substrate temperature variation are presented in graphical form in Figures 1, 2, and 3. These graphs show the distribution of diffraction peaks that characterize the material's crystal structure. By comparing the diffractograms, the optimum conditions that produce the best crystal structure can be analyzed. This information is crucial in determining the quality of the material as a candidate absorber in solar cells. Therefore, XRD analysis is a key step in this research.

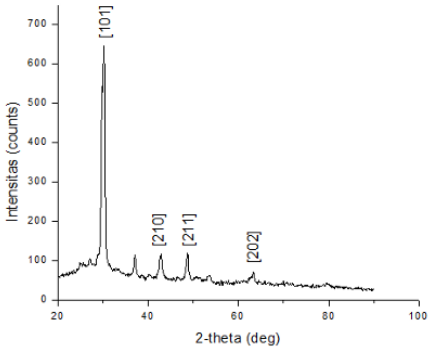

Figure 1. XRD Difactogram of Sn(S0.6Te0.4) Thin Film with Substrate Temperature of 250ºC

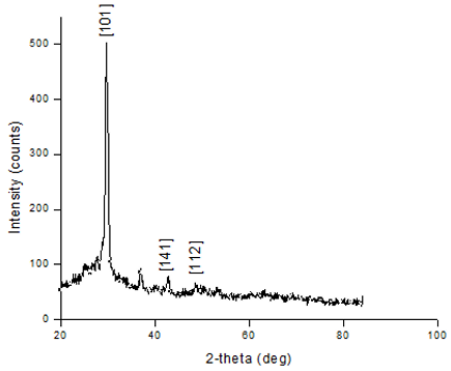

Figure 2. XRD Difactogram of Sn(S0.6Te0.4) Thin Film with Substrate Temperature of 300ºC

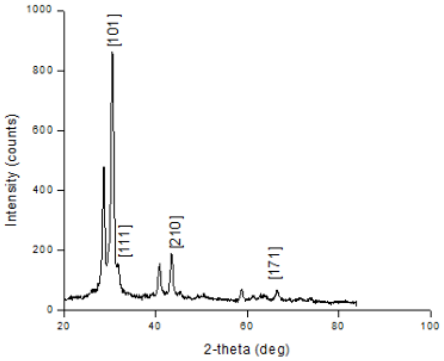

Figure 3. XRD Difactogram of Sn(S0.6Te0.4) Thin Film with Substrate Temperature of 350ºC

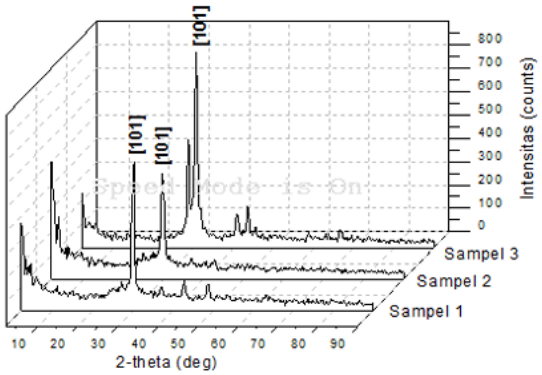

Figure 4. XRD Results of Sn(S0.6Te0.4) Thin Film for Sample 1, Sample 2 and Sample 3

The three prepared samples were analyzed comparatively by combining the diffractogram data using Origin software. This merging facilitates comparison of the diffraction peak characteristics of each sample. Based on the results shown in Figure 4, the main difference lies in the intensity of the resulting diffraction peaks. The sample with a substrate temperature of 350°C exhibited the highest peak intensity, particularly at a diffraction angle (2θ) of approximately 30°. Meanwhile, the samples at temperatures of 250°C and 300°C had relatively lower intensities.

This difference in intensity indicates the level of atomic order in the thin film's crystal structure. The higher the intensity of the diffraction peak, the better the atomic order in the material. Therefore, the sample prepared at 350°C had the highest degree of crystallinity compared to the other samples. This indicates that increasing the substrate temperature has a positive effect on the quality of the crystal structure. Therefore, a temperature of 350°C can be considered the optimum condition for the preparation of $Sn(S_{0.6}Te_{0.4})$ thin films.

To determine the crystal lattice parameters, the initial step is to identify the Miller index (hkl) of each diffraction peak. The (hkl) value is determined by matching the measured diffraction angle (2θ) with standard data from the JCPDS database. This process allows the identification of the crystal planes contributing to the observed diffraction peaks. By knowing the Miller index, the crystal lattice parameters can be calculated analytically. This step is a crucial step in quantitatively understanding the crystal structure of the material.

In searching for JCPDS standard data, PCPDFWIN software was used to obtain appropriate references. Based on the standard data, it was found that SnS has an orthorhombic crystal structure. The orthorhombic crystal system is characterized by different lattice parameters along each axis ($a \neq b \neq c$) and an angle between the axes $\alpha = \beta = \gamma = 90°$. The agreement between the experimental data and standard data indicates that the crystal structure of the formed thin film is close to the structure of SnS. The matching data are then presented in tabular form for each sample, which can be seen in Table 1, Table 2, Table 3.

Table 1. Comparison of XRD Data of Sn(S0,6Te0,4) Thin Film Research Sample 1 (250°C) with JCPDS Data of SnS and SnTe Materials

Peak	Sn(S0,6Te0,4) Sampel 1		SnS JCPDS	SnTe JCPDS	hkl SnS	hkl SnTe
	2θ (°)	I (%)	2θ (°)	2θ (°)		
1	29.638	45.31	-	-	-	-
2	30.231	100	30.472	-	101	-
3	37.057	10.26	-	-	-	-
4	42.81	15.73	42.504	-	210	-
5	48.71	11.64	48.507	-	211	-
6	63.29	7.0	63.387	-	202	-

Table 2. Comparison of XRD Data of Sn(S0,6Te0,4) Thin Film Research Sample 2 (300°C) with JCPDS Data of SnS and SnTe Materials

Peak	Sn(S0,6Te0,4) Sampel 1		SnS JCPDS	SnTe JCPDS	hkl SnS	hkl SnTe
	2θ (°)	I (%)	2θ (°)	2θ (°)		
1	29.74	100	-	-	101	-
2	36.83	4.38	-	-	-	-
3	42.7579	7.97	44.737	-	141	-
4	48.8737	4.75	51.084	-	112	-

Table 3. Comparison of XRD Data of Sn(S0,6Te0,4) Thin Film Research Sample 3 (350°C) with JCPDS Data of SnS and SnTe Materials

Peak	Sn(S0,6Te0,4) Sampel 1		SnS JCPDS	SnTe JCPDS	hkl SnS	hkl SnTe
	2θ (°)	I (%)	2θ (°)	2θ (°)		
1	28.626	35.92	-	28.307	-	200
2	30.507	100	30.472	-	101	-
3	31.64	32.70	31.530	-	111	-
4	40.78	11.71	-	40.413	-	220
5	43.47	16.86	42.504	-	210	-
6	66.61	3.002	66.560	66.224	171	420

Based on the data in the table obtained, the lattice parameters and crystal structure of the $Sn(S_{0.6}Te_{0.4})$ thin film can be determined through analytical calculations. These calculations refer to the basic principle of X-ray diffraction, explained by Bragg's Law. This principle states that diffraction patterns are formed by the interaction between X-rays and crystal planes in a material. Thus, information about the distance between crystal planes can be calculated from the resulting diffraction angles. This makes XRD the primary method for crystal structure analysis.

The relationship between diffraction angle, wavelength, and crystal plane distance follows the following Bragg's Law equation:

$$n\lambda = 2d\sin\,\theta$$

Using this equation, the distance between crystal planes (d) can be calculated based on the diffraction angle (2θ) obtained from the experimental results. This d value is then used in a further equation to determine the crystal lattice parameters. The lattice parameter calculations are performed using equations appropriate to the resulting crystal system [31]. In this study, we used equations for the orthorhombic crystal system because the resulting structure is based on standard SnS data. Using this approach, the lattice parameter values a, b, and c were obtained for each sample.

The analytical lattice parameter calculations were then compared with standard data from the JCPDS database for SnS. This comparison aims to determine the degree of agreement between the resulting crystal structure and existing references. If the obtained lattice parameter values are close to the standard data, it can be concluded that the resulting crystal structure conforms to the orthorhombic structure of SnS. Furthermore, differences in values may indicate the influence of Te substitution in the crystal structure. Therefore, this analysis provides important information regarding structural changes due to compositional variations.

The calculated lattice parameter values and their comparison with the JCPDS data are presented in tabular form for ease of interpretation. These data demonstrate a trend in lattice parameter changes due to variations in preparation conditions. Therefore, these analysis results can be used to evaluate the crystal structure quality of $Sn(S_{0.6}Te_{0.4})$ thin films. Furthermore, this information also supports the determination of the best material as an absorber candidate for solar cell applications.

Table 4. Comparison of Lattice Parameter Values of Sn(S0.6Te0.4) Thin Films from XRD Characterization with JCPDS SnS Data

Grid parameters	Sample Sn(S0,6Te0,4)			JCPDS Sn(S0,6Te0,4)
	1	2	3	
a (Å)	4.30	4.29	4.23	4.329
b (Å)	10.4	11.9	11.19	11.19
c (Å)	4.01	4.19	4.03	3.983

Based on Table 4, the lattice parameters a, b and c of Sn(S0,6Te0,4) can be seen from the research results and JCPDS data for SnS. Of the three samples, there is no significant difference in the lattice parameters, this indicates that variations in substrate temperature do not affect the lattice, but affect the relative intensity.

3.2. Characterization of the Chemical Composition of Sn(S0.6Te0.4) Thin Films by Energy Dispersive Spectroscopy (EDS)

EDS is a tool used to determine the chemical composition of a material. In EDS characterization, the thin layer tested was a thin layer of Sn(S0,6Te0,4) sample 3 with a substrate temperature of 350ºC. Characterization using EDS was carried out after the crystals were characterized using XRD. The results of EDS performed on a thin layer of Sn(S0,6Te0,4) sample 3 can be seen in Figure 5.

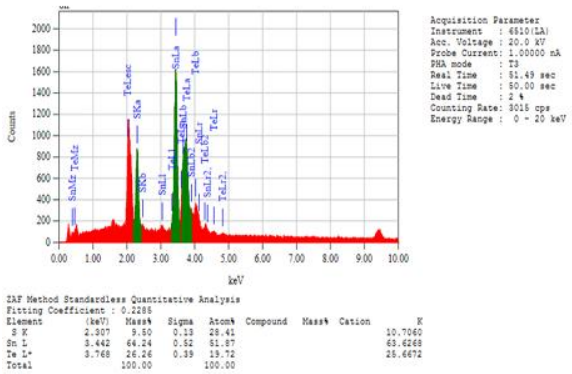

Figure 5. Graph between Intensity and Energy of EDS Characterization Results of Sn(S0.6Te0.4) Thin Films

Based on Figure 5, it can be seen that the preparation of thin film semiconductor crystals Sn(S0,6Te0,4) contains Stannum (Sn), Sulfur (S), and Tellurium (Te) elements. The comparison of the percentage composition of the basic materials, namely the elements Sn = 51.87%, S = 28.41%, Te = 19.72%. The comparison of 66 elemental compositions of Sn(S0,6Te0,4) semiconductor crystals resulting from EDS characterization with theory can be seen in Table 5.

Table 5. Comparison of Molarity of Sn : S : Te Elements in Sn(S0.6Te0.4) Semiconductor Crystals from EDS Characterization Results and Theory

	Sn	S	Te
According to EDS Research	1	0.55	0.38
In Theory	1	0.6	0.4

Based on Table 5, it can be seen that the elemental composition of Sn(S0,6Te0,4) as a result of EDS characterization has a mole ratio of each material Sn: S: Te, namely 1: 0.55: 0.38. While according to the theory, it is 1: 0.6: 0.4. The results of EDS characterization show that the results of the chemical composition from the EDS analysis compared to the theory indicate that there is a change in the atomic composition of S and Te. This discrepancy can indicate that the crystals grown experience a non-stoichiometric event. Non-stoichiometric events can occur during the vacuum process, when the material evaporates from the crucible to the substrate does not adhere perfectly.

XRD characterization results indicate that increasing substrate temperature significantly affects the quality of the resulting Sn($S_{0.6}Te_{0.4}$) crystals. The increase in diffraction peak intensity at 350°C indicates increased atomic order in the crystal structure. Physically, this can be explained by the fact that higher temperatures provide sufficient kinetic energy for atoms to move and occupy more stable lattice positions. Thus, the atomic diffusion process during deposition is more optimal, resulting in a more regular and homogeneous crystal structure. Furthermore, the tendency of the crystal structure to approach the orthorhombic SnS system indicates that the substitution of Te into the lattice does not significantly alter the basic structure but rather affects the material's electronic parameters. This indicates that Sn($S_{0.6}Te_{0.4}$) is a structurally stable alloy, potentially maintaining good mechanical properties and thermal stability. This structural stability is a critical factor in solar cell applications, as absorber materials must be able to operate under varying environmental conditions without experiencing structural degradation.

In terms of lattice parameters, the results showed no significant changes in the a, b, and c values despite variations in substrate temperature [32], [33]. This indicates that temperature plays a greater role in increasing crystallinity than in changing the underlying crystal structure. In other words, the deposition process within the temperature range used remains within the stability limits of the material's crystal structure. However, the slight variation in lattice parameter values can be attributed to the partial substitution effect of Te for S, which causes minor distortions in the crystal lattice due to differences in atomic radii. EDS characterization results confirm the finding that the resulting material contains the main elements Sn, S, and Te with a composition close to the theoretical value. However, the compositional deviation indicates a non-stoichiometric phenomenon during the deposition process. This is likely due to differences in the evaporation rates of each element, where elements with higher vapor pressures tend to evaporate more easily and are not completely deposited evenly on the substrate [34], [35]. This condition is common in vacuum evaporation methods and presents a challenge in achieving a composition that accurately matches the initial design.

This non-stoichiometric phenomenon also has implications for the optical and electronic properties of the material. Compositional imbalances can lead to the formation of crystal defects (defect states), which affect the material's band gap and conductivity [36]. In the context of solar cell applications, the presence of these defects can be positive or negative, depending on their type and concentration. Therefore, compositional control is a crucial aspect in optimizing material performance as an absorber. Overall, the results of this study indicate that substrate temperature and compositional control play key roles in determining the quality of Sn($S_{0.6}Te_{0.4}$) thin films. The combination of a favorable crystal structure, a composition close to stoichiometry, and potentially suitable optical properties make this material a promising candidate for solar cell applications [37], [38]. However, to achieve optimal performance, further development is needed, particularly in controlling the deposition process and improving layer homogeneity.

This research has significant implications for the development of alternative materials for solar cell applications, particularly through the exploration of Sn($S_{0.6}Te_{0.4}$) thin films as potential absorber candidates. The results show that substrate temperature control can enhance the material's crystallinity, while the combination of S and Te elements provides flexibility in engineering the material's properties. These findings contribute to the development of chalcogenide-based materials that are more efficient, stable, and potentially more environmentally friendly than conventional materials [39], [40]. Furthermore, this research provides a more comprehensive understanding of the relationship between crystal structure and chemical composition on the quality of the resulting thin films.

However, this research has several limitations that should be considered. The synthesis process was conducted at a laboratory scale and therefore does not fully represent industrial-scale production conditions. Furthermore, control over the material composition was not optimal, as evidenced by stoichiometric deviations in the EDS results due to differences in the evaporation rates of each element. This research also did not include direct analysis of optical and electrical properties, which are critical parameters in determining the performance of a material as a solar cell absorber. Therefore, further research is needed to optimize deposition parameters, improve composition homogeneity, and assess material performance in real-world photovoltaic device applications.

4. CONCLUSION

Based on the research results, Sn($S_{0.6}Te_{0.4}$) thin films were successfully synthesized using the vacuum evaporation method with substrate temperature variations of 250°C, 300°C, and 350°C. The XRD characterization results showed that increasing the substrate temperature increased the intensity of the diffraction peaks, which indicated an increase in crystallinity, with the optimum condition obtained at a temperature of 350°C. The crystal structure formed approached the orthorhombic SnS system with lattice parameters that did not change significantly with temperature variations. EDS analysis showed that the elemental composition was close to the theoretical value, although there was a slight deviation due to non-stoichiometric phenomena during the deposition process. Overall, Sn($S_{0.6}Te_{0.4}$) material has potential as an absorber in solar cells, and further research can be focused on optimizing the composition and improving the quality of the coating to increase the efficiency of photovoltaic

applications. Further research is recommended to examine the optical and electrical properties of $Sn(S_{0.6}Te_{0.4})$ thin films to directly evaluate their performance as absorber materials in solar cells. Furthermore, more precise optimization of deposition parameters and composition control, as well as device-scale testing, are needed to improve material efficiency and stability.

ACKNOWLEDGEMENTS

The authors would like to express their sincere gratitude to all parties who have supported this research. Special thanks are addressed to the laboratory staff and the Department of Science Education, Universitas Jambi, for providing facilities and technical assistance during the experimental process. The authors also appreciate the academic support and guidance from colleagues and reviewers who contributed valuable insights to improve this study.

AUTHOR CONTRIBUTIONS

For research articles with several authors, a short paragraph specifying their individual contributions must be provided. The following statements should be used "Conceptualization, X.X. and Y.Y.; Methodology, X.X.; Software, X.X.; Validation, X.X., Y.Y. and Z.Z.; Formal Analysis, X.X.; Investigation, X.X.; Resources, X.X.; Data Curation, X.X.; Writing – Original Draft Preparation, X.X.; Writing – Review & Editing, X.X.; Visualization, X.X.; Supervision, X.X.; Project Administration, X.X.; Funding Acquisition, Y.Y.".

CONFLICTS OF INTEREST

The authors declare no conflict of interest.

USE OF ARTIFICIAL INTELLIGENCE (AI)-ASSISTED TECHNOLOGY

Not applicable.

REFERENCES

[1] A. G. Olabi and M. A. Abdelkareem, "Renewable energy and climate change," *Renew. Sustain. Energy Rev.*, vol. 158, no. 112111, pp. 1–21, Apr. 2022, doi: 10.1016/j.rser.2022.112111.

[2] P. F. Borowski, "Mitigating climate change and the development of green energy versus a return to fossil fuels due to the energy crisis in 2022," *Energies*, vol. 15, no. 24, pp. 1–16, 2022, doi: 10.3390/en15249289.

[3] M. Dada and P. Popoola, "Recent advances in solar photovoltaic materials and systems for energy storage applications: a review," *Beni-Suef Univ. J. Basic Appl. Sci.*, vol. 12, no. 66, pp. 1–15, 2023, doi: 10.1186/s43088-023-00405-5.

[4] M. Ashraf *et al.*, "Recent trends in sustainable solar energy conversion technologies: Mechanisms, prospects, and challenges," *Energy & Fuels*, vol. 37, no. 9, pp. 6283–6301, May 2023, doi: 10.1021/acs.energyfuels.2c04077.

[5] J. Dhilipan, N. Vijayalakshmi, D. B. Shanmugam, R. Jai Ganesh, S. Kodeeswaran, and S. Muralidharan, "Performance and efficiency of different types of solar cell material – A review," *Mater. Today Proc.*, vol. 66, pp. 1295–1302, 2022, doi: 10.1016/j.matpr.2022.05.132.

[6] M. K. Hossain *et al.*, "Exploring the optoelectronic and photovoltaic characteristics of lead-free Cs2TiBr6 double perovskite solar cells: A DFT and SCAPS-1D investigations," *Adv. Electron. Mater.*, vol. 11, no. 2, pp. 1–18, 2025, doi: 10.1002/aelm.202400348.

[7] P. Priyadarshini, S. Das, and R. Naik, "A review on metal-doped chalcogenide films and their effect on various optoelectronic properties for different applications," *RSC Adv.*, vol. 12, no. 16, pp. 9599–9620, 2022, doi: 10.1039/d2ra00771a.

[8] P. Pimpang, K. Hongsith, S. Choopun, and S. Wongrerkdee, "A review on chalcogenide-based materials for counter electrode applications in dye-sensitized solar cells: Sulfides, selenides, and tellurides," *ACS Omega*, vol. 10, no. 25, pp. 26293–26310, Jul. 2025, doi: 10.1021/acsomega.5c03194.

[9] A. Rani, W. Ren, H. J. Lee, S. H. Hong, and T. G. Kim, "Synthesis, properties, and application of ultrathin and flexible tellurium nanorope films: Beyond conventional 2D materials," *Small*, vol. 20, no. 1, pp. 1–10, 2024, doi: 10.1002/smll.202300557.

[10] A. K. Katiyar *et al.*, "2D materials in flexible electronics: Recent advances and future prospectives," *Chem. Rev.*, vol. 124, no. 2, pp. 318–419, Jan. 2024, doi: 10.1021/acs.chemrev.3c00302.

[11] P. Xu, X. Ji, M. Li, and W. Lu, "Small data machine learning in materials science," *npj Comput. Mater.*, vol. 9, no. 1, pp. 1–15, 2023, doi: 10.1038/s41524-023-01000-z.

[12] R. Baskara and M. Mukarto, "Exploring the implications of ChatGPT for language learning in higher education," *Indones. J. English Lang. Teach. Appl. Linguist.*, vol. 7, no. 2, pp. 343–358, 2023, doi: 10.21093/ijeltal.v7i2.1387.

[13] A. M. Adeyinka, O. V. Mbelu, Y. B. Adediji, and D. I. Yahya, "A review of current trends in thin film solar cell technologies," *Int. J. Energy Power Eng.*, vol. 17, no. 1, pp. 1–10, 2023.

[14] S. Rubin, D. Mizrachi, N. Friedman, H. Edri, and T. Golan, "The world of advanced thin Films: design, fabrication, and applications," *Fusion Multidiscip. Res. An Int. J.*, vol. 4, no. 1, pp. 393–406, 2023, doi: 10.63995/sikh4721.

[15] T. Nimalan and M. R. Begam, "Physical and chemical Methods: A review on the analysis of deposition parameters of thin film preparation methods," *Int. J. Thin Film Sci. Technol.*, vol. 13, no. 1, pp. 59–66, 2024, doi: 10.18576/ijtfst/130107.

[16] T. Bai, S. Wang, L. Bai, K. Zhang, C. Chu, and L. Yi, "Vacuum evaporation of high-quality CsPbBr3 thin films for efficient light-emitting diodes," *Nanoscale Res. Lett.*, vol. 17, no. 1, pp. 1–11, 2022, doi: 10.1186/s11671-022-03708-1.
[17] H. Jeong, G. Park, J. Jeon, and S. S. Park, "Fabricating large-area thin films of 2D conductive metal–organic frameworks," *Acc. Chem. Res.*, vol. 57, no. 16, pp. 2336–2346, Aug. 2024, doi: 10.1021/acs.accounts.4c00292.
[18] M. A. Butt *et al.*, "Optical thin films fabrication techniques—towards a low-Cost solution for the integrated photonic platform: A review of the current status," *Materials (Basel).*, vol. 15, no. 13, pp. 1–25, 2022, doi: 10.3390/ma15134591.
[19] E. Kaya and B. Coşkun, "An overview for fundamental chemical characterization techniques for thin films and nanostructures," *J. Mater. Electron. Devices*, vol. 2, no. 1, pp. 19–24, 2024, [Online]. Available: https://www.dergi-fytronix.com/index.php/jmed/article/view/266
[20] K. Shahzad, A. I. Mardare, and A. W. Hassel, "Accelerating materials discovery: combinatorial synthesis, high-throughput characterization, and computational advances," *Sci. Technol. Adv. Mater. Methods*, vol. 4, no. 1, pp. 1–42, 2024, doi: 10.1080/27660400.2023.2292486.
[21] J. L. Pura, "Optical and electrical properties of low-dimensional crystalline materials: A review," *Crystals*, vol. 13, no. 1, pp. 1–18, 2023, doi: 10.3390/cryst13010108.
[22] F. Li *et al.*, "Modulation of the lattice structure of 2D carbon-based materials for improving photo/electric properties," *Carbon Lett.*, vol. 33, no. 5, pp. 1321–1331, Aug. 2023, doi: 10.1007/s42823-022-00380-4.
[23] M. I. Rodríguez-Tapiador *et al.*, "Effects of deposition temperature and working pressure on the thermal and nanomechanical performances of stoichiometric Cu3N: An adaptable material for photovoltaic applications," *Nanomaterials*, vol. 13, no. 22, pp. 1–19, 2023, doi: 10.3390/nano13222950.
[24] C. Tsounis *et al.*, "Advancing mxene electrocatalysts for energy conversion reactions: Surface, stoichiometry, and stability," *Angew. Chemie - Int. Ed.*, vol. 62, no. 4, pp. 1–20, 2023, doi: 10.1002/anie.202210828.
[25] S. A. Essaa and H. R. Jappor, "Tunable photocatalytic and optoelectronic properties of SiTe/SiH heterostructure as a photocatalytic water splitting with high hydrogen production," *J. Phys. Chem. Solids*, vol. 193, p. 112125, Oct. 2024, doi: 10.1016/j.jpcs.2024.112125.
[26] S. Wang, Z. Song, and Q. Liu, "Recent progress in Ce 3+ /Eu 2+ -activated LEDs and persistent phosphors: focusing on the local structure and the electronic structure," *J. Mater. Chem. C*, vol. 11, no. 1, pp. 48–96, 2023, doi: 10.1039/D2TC02639B.
[27] Y. Liang, X. Wei, Y. Peng, X. Wang, and X. Niu, "A review on recent applications of machine learning in mechanical properties of composites," *Polym. Compos.*, vol. 46, no. 3, pp. 1939–1960, Feb. 2025, doi: 10.1002/pc.29082.
[28] X. Zhong, B. Gallagher, S. Liu, B. Kailkhura, A. Hiszpanski, and T. Y. J. Han, "Explainable machine learning in materials science," *npj Comput. Mater.*, vol. 8, no. 1, pp. 1–19, 2022, doi: 10.1038/s41524-022-00884-7.
[29] E. A. Pecherskaya, A. D. Semenov, T. O. Zinchenko, A. A. Danilov, and D. E. Tuzova, "The system of automatic control of the substrate temperature as part of the installation for the production of film material by spray pyrolysis," *Meas. Tech.*, vol. 67, no. 5, pp. 377–385, Aug. 2024, doi: 10.1007/s11018-024-02357-3.
[30] C. Shen *et al.*, "Vacuum thermal evaporation for OLEDs: Fundamentals, optimization, and implications for perovskite LEDs," *Adv. Electron. Mater.*, vol. 11, no. 19, pp. 1–26, 2025, doi: 10.1002/aelm.202500555.
[31] M. Kawsar, M. S. Hossain, N. M. Bahadur, and S. Ahmed, "Synthesis of nano-crystallite hydroxyapatites in different media and a comparative study for estimation of crystallite size using Scherrer method, Halder-Wagner method size-strain plot, and Williamson-Hall model," *Heliyon*, vol. 10, no. 3, pp. 1–14, 2024, doi: 10.1016/j.heliyon.2024.e25347.
[32] S. Pedrazzini *et al.*, "Effect of substrate bed temperature on solute segregation and mechanical properties in Ti–6Al–4V produced by laser powder bed fusion," *Metall. Mater. Trans. A Phys. Metall. Mater. Sci.*, vol. 54, no. 8, pp. 3069–3085, 2023, doi: 10.1007/s11661-023-07070-4.
[33] S. K. Ryoo *et al.*, "Investigation of optimum deposition conditions of radio frequency reactive magnetron sputtering of Al 0.7 Sc 0.3 N film with thickness down to 20 nm," *Adv. Electron. Mater.*, vol. 8, no. 11, pp. 1–15, Nov. 2022, doi: 10.1002/aelm.202200726.
[34] X. Wang *et al.*, "Electrified vapour deposition at ultrahigh temperature and atmospheric pressure for nanomaterials synthesis," *Nat. Synth.*, vol. 5, no. 1, pp. 14–26, 2026, doi: 10.1038/s44160-025-00914-4.
[35] F. V. E. Hensling *et al.*, "State of the art, trends, and opportunities for oxide epitaxy," *APL Mater.*, vol. 12, no. 4, pp. 1–13, Apr. 2024, doi: 10.1063/5.0196883.
[36] S. Bera *et al.*, "Review of defect engineering in perovskites for photovoltaic application," *Mater. Adv.*, vol. 3, no. 13, pp. 5234–5247, 2022, doi: 10.1039/d2ma00194b.
[37] Y. Zhang, Y. Liu, and S. (Frank) Liu, "Composition engineering of perovskite single crystals for high-performance optoelectronics," *Adv. Funct. Mater.*, vol. 33, no. 9, pp. 1–15, Feb. 2023, doi: 10.1002/adfm.202210335.
[38] N. S. Seroka, R. Taziwa, and L. Khotseng, "Solar energy materials-evolution and niche applications: A literature review," *Materials (Basel).*, vol. 15, no. 15, pp. 1–18, 2022, doi: 10.3390/ma15155338.
[39] M. O. Alfred, E. Akor, B. C. Ayeni, C. G. Olorunnisola, E. I. Unuabonah, and M. O. Omorogie, "Chalcogenides: recent advances in their environmental applications," *Energy, Ecol. Environ.*, vol. 11, pp. 10–38, 2025, doi: 10.1007/s40974-025-00389-1.
[40] D. C. Akintayo, T. L. Yusuf, and N. Mabuba, "Chalcogenide materials in water purification: Advances in adsorptive and photocatalytic removal of organic pollutants," 2025. doi: 10.1002/smll.202501378.